

# Theoretical Model and Experimental Research on Mortar Corrosion by Sulfuric Acid in Laminar Flow

Weihang ZHANG, Zhigang SONG\*

**Abstract:** Surfaces of concrete structure could suffer the corrosion of flowing sulfuric acid coming from acid rain or sewage water. This paper establishes an analytical corrosion model and carries out experimental studies to investigate the corrosion rate of mortar in laminar flow of sulfuric acid with different flow velocities. The analytical model was deduced from the relationship between Flow Boundary Layer and Concentration Boundary Layer, connected by Schmidt number, and the dissolution diffusion process of mortar. The analytical model indicates that the corrosion rate will increase with flow velocity, but the increment effect will decrease with flow velocity in an exponential relationship. Nine groups of cement mortar specimens were tested in flow-corrosion devices for 1440 hours. The corrosion rate was obtained for the cases of the water cement ratio of mortar 0.5, the pH value of sulfuric acid 3.4 and the flow velocities ranging from 0.13 m/s to 1.57 m/s.

**Keywords:** cement mortar; flow-corrosion model; laminar flow; sulfuric acid

## 1 INTRODUCTION

With the wide use of concrete and the development of industrialization, the aging of concrete due to sulfuric acid, which is produced by air pollution [1-4], industrial production [5-8] and microbial activity [9-13], has become a global issue. According to the ways of the sulfuric acid acting on the structure, the acting modes can generally be classified as static mode and flowing mode. Song et al. [14] classified the corrosion zones on the surface of concrete structure into three types, namely direct acting zone, confluence acting zone and retention acting zone, through field investigation. Thistlethwayte et al. [15] researched the sulfuric acid corrosion caused by microbial activities in concrete sewage pipe, and classified corrosion parts in sewage pipe into gas phase region and gas-liquid junction area. Both acid rain detention zone and gas phase region suffered static sulfuric acid corrosion, which had been widely studied through experimental and/or theoretical approaches. Israel et al. [16] found different corrosion laws among sulfuric acid, hydrochloric acid and nitric acid based on immersion test. Zhou et al. [17] confirmed the different corrosion mechanism between sulfuric acid and sulfate. Hewayde et al. [18] studied the influences of concrete mixture ratio and other additives, such as silica fume, high ridge soil and organic anti-penetrating materials, on anti-sulphate ability of concrete. Xie et al. [19] found the growth of laws of the neutralization depth of concrete over time. Bohm et al. [20] proposed a moving boundary diffusion model to predict the corrosion rate, and confirmed parameters that influence the corrosion rate. Liu et al. [21] deduced the diffusion equation of sulfuric acid solution in cylinder specimen, and suggested the relationship between corrosion quantity and time based on Fick's law. Song et al. [22] proposed a sulfuric acid corrosion model about acid consumption rate based on boundary layer theory. However, there are relatively fewer studies focusing on concrete structure corroded by flowing sulfuric acid and which, as mentioned above, is a typical acting mode in direct acting zone, confluence acting zone and gas-liquid junction area.

The paper studies the theoretical model of mortar corrosion in flowing sulfuric acid under the laminar flow

conditions through the boundary layer theory. Firstly, the thickness of flow boundary layer (FBL) near the cement mortar surface was achieved by laminar flow theory and based on which the thickness of concentration boundary layer (CBL) of reactants could be deduced with the help of Schmidt law. Thus, the concentration gradients of reactants in concentration boundary layer could be determined and furthermore, the corrosion rate could be deduced through the two order homogeneous chemical reaction diffusion equations. Finally, a theoretical relationship describing corrosion rate of the mortar and flow velocity of sulfuric acid is proposed. To verify the validities of the model, 9 groups of cement mortar specimens were tested in flow-corrosion devices for 1440 hours. The corrosion rate was obtained for the cases of water cement ratio of mortar 0.5, the pH value of sulfuric acid 3.4 and the flow velocities ranging from 0.13 m/s to 1.57 m/s.

## 2 MODEL OF MORTAR CORROSION IN FLOWING SULFURIC ACID

### 2.1 FBL and CBL

When sulfuric acid flows over the mortar surface, there exists a velocity gradient, namely FBL, in fluid thin layer adjacent to the surface due to the viscous effect. According to Blasius [23], the thickness  $\delta_v(u)$  of FBL in laminar flow could be expressed as:

$$\delta_v(u) = 5\sqrt{\nu L / u} \quad (1)$$

where  $\nu$  is coefficient of kinematic viscosity ( $\text{m}^2/\text{s}$ ),  $L$  is feature size (m),  $u$  is fluid velocity (m/s).

Meanwhile, there is also a concentration gradient vertical to flowing direction because of the chemical reaction and mass transformation in the interface of the mortar and sulfuric acid. Therefore, two boundary layers, i.e. FBL and CBL, simultaneously exist on surface of mortar as the dilute sulfuric acid flowing passes the mortar surface (Fig. 1). According to Schmidt's law, the relationship between the thickness of CBL  $\delta_c(u)$  and the thickness of FBL  $\delta_v(u)$  in the laminar flow is [24]

$$\delta_c(u) / \delta_v(u) = Sc^{-1/3} \quad (2)$$

where,  $Sc$  is the Schmidt number. Combining Eq. (1) and Eq. (2), we can have

$$\delta_c(u) = 5u^{-1/2} Sc^{-1/3} \sqrt{\nu L} \quad (3)$$

From Eq. (3), it is found that the thickness of CBL will decrease with the increase of flow velocity. And this, by increase of the concentration gradient and diffusion flux of sulfuric acid, can finally strengthen the corrosion of dilute sulfuric acid.

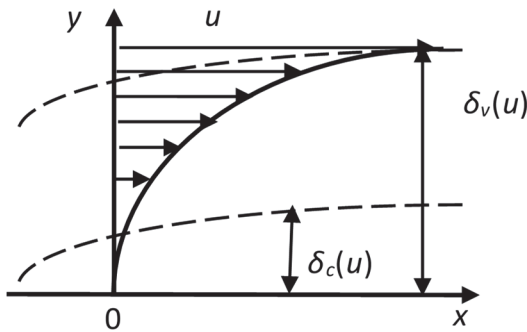


Figure 1 Concentration boundary layer and flow boundary layer

## 2.2 Process of Dilute Sulfuric Acid Eroding Mortar

The chemical reaction of the corrosion is a process in which the hydration products of cement mortar dissolve out and then are continuously consumed by the acid. The CBL near the mortar surface is shown in Fig. 2.

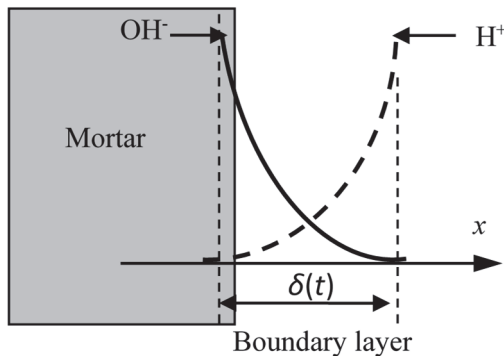


Figure 2 Concentration boundary layer between acid and mortar

The process can be modeled by a two order homogeneous chemical reaction diffusion equation of  $OH^-$  in CBL:

$$\frac{\partial C_{OH^-}(x,t)}{\partial t} = D_{OH^-} \frac{\partial^2 C_{OH^-}(x,t)}{\partial x^2} - kC_{OH^-}(x,t)C_{H^+}(x,t) \quad (4)$$

where,  $x$  is the distance to the fresh surface(m),  $t$  is reaction time (s),  $C_{OH^-}(x,t)$  and  $C_{H^+}(x,t)$  are concentration of  $OH^-$  and  $H^+$  at time  $t$  and location  $x$  respectively (mol/L),  $D_{OH^-}$  is the diffusion coefficient of  $OH^-$  in boundary layer ( $m^2/s$ ),  $k$  is a reaction constant ( $mol^{-1}s^{-1}$ ).

Boundary condition:

$$\begin{cases} x = 0, C_{OH^-}(0,t) = C_{OH^-,s}, C_{H^+}(0,t) = 0 \\ x = \delta(t), C_{OH^-}(\delta(t),t) \approx 1\%C_{OH^-,s}, C_{H^+}(\delta(t),t) \approx 99\%C_{H^+,s} \end{cases} \quad (5)$$

where  $C_{OH^-,s}$  is the concentration of  $OH^-$  in saturated solution of  $Ca(OH)_2$  and  $C_{H^+,s}$  is the concentration of  $H^+$  in dilute sulfuric acid.  $\delta(t)$  (m) is the thickness of boundary layer, and it can be defined as a distance where concentration is reduced to one percent of initial concentration.

## 2.3 Solution under Flowing Acid Conditions

We assume the concentration profile of  $H^+$  and  $OH^-$  satisfies the following form:

$$\begin{aligned} C_{OH^-}(x,t) &= C_{OH^-,s} \exp(-Fx/\delta(t)), C_{H^+}(x,t) = \\ &= C_{H^+,s} [1 - \exp(-Fx/\delta(t))] \end{aligned} \quad (6)$$

Combining Eq. (4) and Eq. (6), we can have

$$\frac{Fx}{\delta(t)^2} \frac{d\delta(t)}{dt} = D_{OH^-} \frac{F^2}{\delta(t)^2} - kC_{H^+,s} [1 - \exp(-Fx/\delta(t))] \quad (7)$$

Integrating both sides of Eq. (7) from 0 to  $\delta(t)$  and by rearrangement, we can have,

$$\frac{Fd\delta(t)}{2dt} = D_{OH^-} \frac{F^2}{\delta(t)} - kC_{H^+,s} (\delta(t) + \frac{\delta(t)}{F} e^{-F} - \frac{\delta(t)}{F}) \quad (8)$$

or

$$\frac{d\delta(t)^2}{4D_{OH^-}F^2 - \frac{4kC_{H^+,s}(F + e^{-F} - 1)}{F^2}} = dt \quad (9)$$

Integrating Eq. (9), we can have,

$$\begin{aligned} \ln(4D_{OH^-}F^2 - \frac{4kC_{H^+,s}(F + e^{-F} - 1)\delta(t)^2}{F^2}) &= \\ &= -\frac{4kC_{H^+,s}(F + e^{-F} - 1)}{F^2}t + C \end{aligned} \quad (10)$$

According to initial condition,  $t = 0$  and  $\delta(t) = 0$ , we can obtain  $C = \ln(4D_{OH^-}F^2)$ . Further, substituting  $C$  into Eq. (10), we can have,

$$\begin{aligned} \delta(t) &= \\ &= \sqrt{4F^2D_{OH^-}(1 - \exp(-\frac{4kC_{H^+,s}(F + \exp(-F) - 1)}{F^2}t))} \end{aligned} \quad (11)$$

The flux of acid over the corrosion area  $S$  is,

$$\begin{aligned} V_{H^+}(t,x) &= D_{H^+}S \frac{\partial C_{H^+}}{\partial x} \Big|_x = \\ &= D_{H^+}C_{H^+,s}S \frac{F}{\delta(t)} \exp(-\frac{Fx}{\delta(t)}) \end{aligned} \quad (12)$$

According to Eq. (3), the thickness of CBL is  $\delta_c(u)$  in the laminar flow of acid. Thus, at  $x = \delta_c(u)$ , the consumption rate  $V_{H^+}(t)$  of acid can be expressed as Eq. (13),

$$V_{H^+}(t, \delta_c(u)) = D_{H^+} S \frac{\partial C_{H^+}}{\partial x} \Big|_{x=\delta_c(u)} = D_{H^+} C_{H^+,S} \frac{F}{\delta(t)} \exp\left(-\frac{F\delta_c(u)}{\delta(t)}\right) \quad (13)$$

Substituting Eq. (3) and Eq. (12) into Eq. (13), we can have

$$V_{H^+}(t, \delta_c(u)) = \frac{a}{\sqrt{1-\exp(-bt)}} \exp\left(-\frac{cu^{-1/2}}{\sqrt{1-\exp(-bt)}}\right) \quad (14)$$

where,

$$\begin{cases} a = \frac{D_{H^+} C_{H^+,S}}{2\sqrt{D_{OH^-}}} \\ b = \frac{4kC_{H^+,S}(F + \exp(-F) - 1)}{F^2} \\ c = \frac{5Sc^{-1/3}\sqrt{\nu L}}{2\sqrt{D_{OH^-}}} \end{cases} \quad (15)$$

From Eq. (14),  $V_{H^+}(t)$  will increase with  $u$  due to  $c > 0$ . Also from Eq. (14), the acid consumption rate  $V_{H^+}(t)$  tended to 0 when  $u$  tended to 0. However, there is no  $\delta_c(u)$  in this case at all. Therefore, the Eq. (14) can merely be applied to explain the law of corrosion rate under the flowing acid condition.

### 2.3 Reaction Rates

It can be seen from Eq. (14), the acid consumption rate at  $t$  can be expressed as Eq. (16) and Eq. (17) when flowing velocities are  $u_0$  and  $u_1$  respectively.

$$V_{H^+}(t, \delta_c(u_0)) = \frac{a}{\sqrt{1-\exp(-bt)}} \exp\left(-\frac{cu_0^{-1/2}}{\sqrt{1-\exp(-bt)}}\right) \quad (16)$$

$$V_{H^+}(t, \delta_c(u_1)) = \frac{a}{\sqrt{1-\exp(-bt)}} \exp\left(-\frac{cu_1^{-1/2}}{\sqrt{1-\exp(-bt)}}\right) \quad (17)$$

The ratio  $R(t)$  between Eq. (17) and Eq. (16) can be expressed as,

$$R(t) = \frac{V_{H^+}(t, \delta_c(u_1))}{V_{H^+}(t, \delta_c(u_0))} = \exp\left(\frac{cu_0^{-1/2} - cu_1^{-1/2}}{\sqrt{1-\exp(-bt)}}\right) \quad (18)$$

As Eq. (18) shows, due to  $c > 0$ , the ratio  $R(t)$  will be bigger than one when  $u_1 > u_0$ , i.e. the acid consumption rate will increase with flow velocity. Further, it can be seen

from Eq. (11) and Eq. (13), for giving flow velocity, the acid consumption rate  $V_{H^+}(t)$  will approach to a certain value (Eq. (19)), when reaction time approaches to infinity.

$$V_{H^+}(t \rightarrow \infty) = \frac{D_{H^+} C_{H^+,S}}{2\sqrt{D_{OH^-}}} \exp\left(-\frac{5u^{-1/2} Sc^{-1/3} \sqrt{\nu L}}{2\sqrt{D_{OH^-}}}\right) = a \exp(-cu^{-1/2}) \quad (19)$$

Eq. (19) indicates that the acid consumption rate  $V_{H^+}(t)$  will tend to a positive constant when the reaction time approaches to infinity. Further, the stable acid consumption rate will increase with the flowing velocity, but, there exists an upper limit value  $a$ . This value is determined by concentration of sulfuric acid, diffusion coefficient of  $H^+$ , and corrosion area of mortar when reaction is stable.

### 2.4 Acid Consumption

Integrating both sides of Eq. (14) from 0 to  $T$ , we can obtain the acid consumption  $M_{H^+}(T)$ ,

$$M_{H^+}(T) = \int_0^T V_{H^+}(t, \delta_c) dt = \int_0^T \frac{a}{\sqrt{1-\exp(-bt)}} \exp\left(-\frac{cu^{-1/2}}{\sqrt{1-\exp(-bt)}}\right) dt \quad (20)$$

Since the integral of Eq. (20) is difficult, a second-order expansion of velocity influence item is introduced to approximate the velocity influence item:

$$V_{H^+}(t, \delta_c(u)) = \frac{a}{\sqrt{1-\exp(-bt)}} \exp\left(-\frac{cu^{-1/2}}{\sqrt{1-\exp(-bt)}}\right) \approx \frac{a}{\sqrt{1-\exp(-bt)}} \left[ 1 - \left(\frac{cu^{-1/2}}{\sqrt{1-\exp(-bt)}}\right) + \frac{1}{2} \left(\frac{cu^{-1/2}}{\sqrt{1-\exp(-bt)}}\right)^2 \right] \quad (21)$$

$$= \frac{a}{\sqrt{1-\exp(-bt)}} - \frac{acu^{-1/2}}{1-\exp(-bt)} + \frac{ac^2u^{-1}}{2[1-\exp(-bt)]^{3/2}}$$

Substitute Eq. (21) into Eq. (20), and integrating both sides of Eq. (20), we can obtain the total acid consumption  $M_{H^+}(T)$  within  $T$ ,

$$M_{H^+}(T) = \int_0^T V_{H^+}(t, \delta_c) dt \approx \int_0^T \left( \frac{a}{\sqrt{1-\exp(-bt)}} - \frac{acu^{-1/2}}{1-\exp(-bt)} + \frac{ac^2u^{-1}}{2[1-\exp(-bt)]^{3/2}} \right) dt \quad (22)$$

$$= \frac{2a}{b} \ln \left[ \frac{1 + \sqrt{1-\exp(-bT)}}{1 - \sqrt{1-\exp(-bT)}} \right] - \frac{acu^{-1/2}}{b} \ln \left( \frac{[\exp(-bT) - 1]}{[\exp(-bT)]} \right) + \frac{acu^{-1}}{b} \left\{ \ln \left[ \left( \sqrt{1-\exp(-bT)} + 1 \right) / \left( \sqrt{1-\exp(-bT)} - 1 \right) \right] - \frac{2}{\sqrt{1-\exp(-bT)}} \right\}$$

$$= A(T) - B(T)u^{-1/2} + C(T)u^{-1}$$

where,

$$\begin{cases} A(T) = \frac{2a}{b} \ln \left\{ \frac{1 + \sqrt{1 - \exp(-bT)}}{1 - \sqrt{1 - \exp(-bT)}} \right\} \\ B(T) = \frac{ac}{b} \ln \left( \frac{\exp(-bT) - 1}{\exp(-bT)} \right) \\ C(T) = \frac{ac}{b} \left\{ \frac{\ln \left[ \frac{(\sqrt{1 - \exp(-bT)} + 1) / \sqrt{1 - \exp(-bT)} - 1}{2} \right]}{-\sqrt{1 - \exp(-bT)}} \right\} \end{cases} \quad (23)$$

As Eq. (22) shows, the acid consumption  $M_{H^+}(T)$  will tend to  $A(T)$  when flow velocity tends to infinite, i.e. the corrosion amount would not always increase with flow velocity, and there exists an upper limit.

### 3 EXPERIMENTS

#### 3.1 Materials

Ten cylindrical cement mortar specimens (50 mm in diameter × 100 mm in height) were manufactured according to Ref [25]. Mixing materials include Portland cement (Grade P.0.42.5), China ISO standard sand based on ISO679&EN196-1, distilled water and the mix proportion, see Tab. 1.

#### 3.2 Flow-Corrosion Devices

A flow-corrosion device mainly composed by electrical rotation engine, tank, energy dissipation mesh and velocity controller was made to simulate the flow-corrosion process, see Fig. 3.

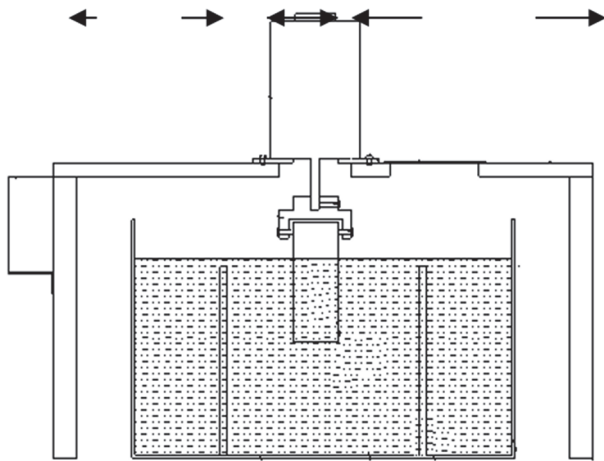


Figure 3 Flow-corrosion device

With the controller, the device can provide a rotational linear velocity range from 0 m/s to 3.66 m/s. The critical Reynolds number ( $Re_c$ ) that fluid transits from laminar to turbulent is  $1.5 \times 10^5 \sim 3.5 \times 10^5$ .

$$Re_c = u_c D / \nu \quad (24)$$

where, the diameter of specimen  $D$  is 0.05m, the coefficient of kinematic viscosity  $\nu$  of sulfuric acid is  $1.00374 \times 10^{-6}$  m<sup>2</sup>/s (at 20 °C, standard atmosphere), the critical flowing

velocity  $u_c$  ranges from 3 m/s to 7 m/s. The rotation linear velocity of specimen selected in this test is 0 m/s ~ 1.57 m/s, which belongs to laminar.

#### 3.3 Experimental Arrangement

The experiment factors in consideration are listed in Tab. 1. The mortar was cast in mould and then cured in saturated solution of Ca(OH)<sub>2</sub> for 28 days. After the curing was finished, the specimens were dried indoor for 7 days. Erase the surface laitance layer, coat the top and bottom with the polyvinyl resin and only leave lateral side sides for reaction, see Fig. 4. Corrosion solution (pH = 3.4) was made up by distilled water and concentrated sulfuric acid. The pH value of corrosion solution was measured by pH meter (Model PHB-1 with an accuracy ±0.01 pH unit) and combined electrodes (Model E-201-C). Ten plastic boxes (volume 20 L and size 467 mm × 363 mm × 215 mm) were filled with corrosion solution. After the test begins, pH meter was used to monitor the pH value. At the same time, the titration dilute sulfuric acid with concentration of 0.125 mol/L was used to maintain the pH value. The average reaction rate represented by titration volume can be determined as below:

$$V_{Hi} = V_i (t_i - t_{i-1})^{-1} \quad (25)$$

where,  $t_{i-1}$  and  $t_i$  is the time of the  $i-1$ <sup>th</sup> and  $i$ <sup>th</sup> titration respectively.  $V_i$  is volume consumption of titration acid (concentration 0.125 mol/L) in the  $i$ <sup>th</sup> titration.  $V_{Hi}$  is the average reaction rate between time  $t_{i-1}$  and  $t_i$ .

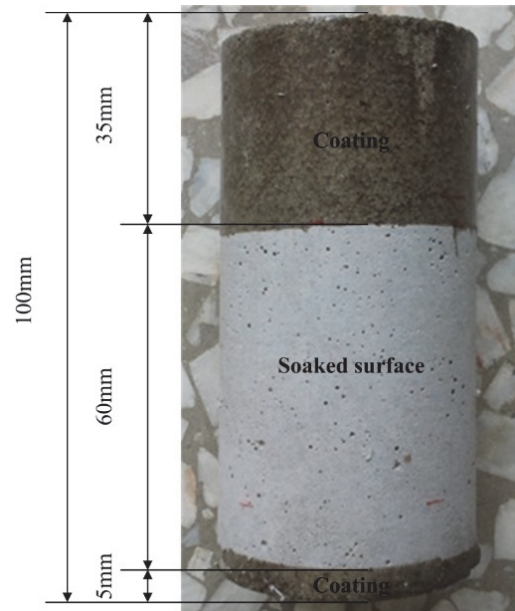


Figure 4 Cement mortar specimen

Table 1 Linear velocity

Group	Linear velocity / m/s
1	0.13
2	0.26
3	0.39
4	0.52
5	0.65
6	0.78
7	1.04
8	1.31
9	1.57

3.4 Results and Discussion

3.4.1 Appearances of Specimens

After 1440 hours, the specimens were taken out and dried indoor for 7 days. Immersed specimens have the following features: (a) Sizes of all specimens decrease to some extent and the immersed surfaces are caved in. But there is no crack observed. (b) The yellow sand layer is observed which is very loose and can be erased by a finger touch.

3.4.2 Acid Consumption  $M_{H^+}(T)$

The total acid consumptions after 600 h, 900 h, 1200 h and 1440 h are listed in Tab. 2. The corresponding  $A(T)$ ,  $B(T)$  and  $C(T)$  fittings according to Eq. (22) are listed in Tab. 3. The fitting curves are plotted in Fig. 5. It is found that Eq. (22) results in a very high degree of fitting. It indicates that the experimental relationship between acid consumption and flow velocity is identical to the theory model perfectly.

Table 2 Acid consumption of the specimen at different times

Group	$u$ / m/s	$M_{H^+}(T)$ / mmol			
		600 h	900 h	1200 h	1440 h
1	0.13	7.02	8.02	8.92	9.74
2	0.26	7.18	8.26	9.16	9.97
3	0.39	7.96	9.27	10.28	11.15
4	0.52	7.99	9.51	10.51	11.39
5	0.65	8.14	9.67	10.68	11.58
6	0.78	8.25	9.91	10.88	11.78
7	1.04	8.85	10.61	11.60	12.53
8	1.31	9.27	10.65	12.09	12.90
9	1.57	9.60	11.35	12.34	13.08

Table 3 Regression results of experiment results according to Eq. (22)

Time	$A(T)$	$B(T)$	$C(T)$	Correlation coefficient
600 h	12.92	5.324	1.258	0.950
900 h	14.10	4.385	0.748	0.951
1200 h	15.76	5.128	0.934	0.967
1440 h	15.99	4.153	0.583	0.971

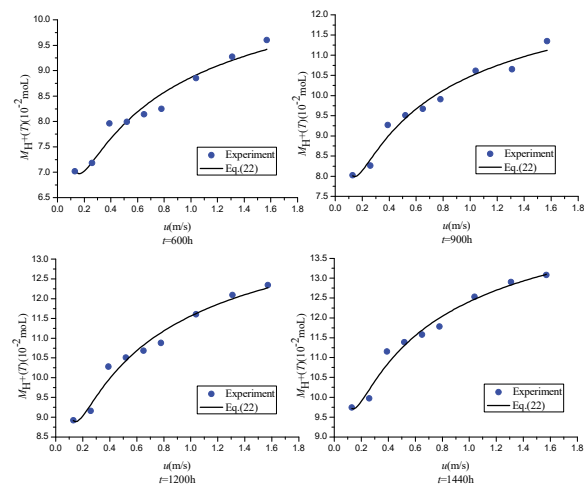


Figure 5 Acid consumption and fitting curves of the specimen at different times

3.4.3 Acid Consumption Rate  $V_{H^+}(t)$

The rates obtained by experiment are fitted according to Eq. (14) and the results of  $a$ ,  $b$  and  $c$  of different groups are listed in Tab. 4. The fitting curves are plotted in Fig. 6.

It is found that Eq. (14) results in a very high degree of fitting.

Table 4 Regression results of experiment results according to Eq. (14)

Group	$a \times 10^3 / \text{m}^3 \text{mol} / \text{h}^{1/2} \text{mL}$	$b \times 10^7 / \text{h}^{-1} \text{mL}^{-1}$	$c \times 10^4 / \text{m}^{1/2}$	Correlation coefficient
1	4.507	3.12	2.605	0.923
2	9.923	11.21	1.442	0.945
3	4.216	2.45	0.616	0.955
4	10.14	10.40	10.62	0.933
5	10.64	11.08	13.17	0.945
6	11.29	12.50	13.78	0.939
7	10.79	10.24	13.02	0.953
8	10.90	9.55	11.38	0.953
9	11.50	9.98	11.96	0.964

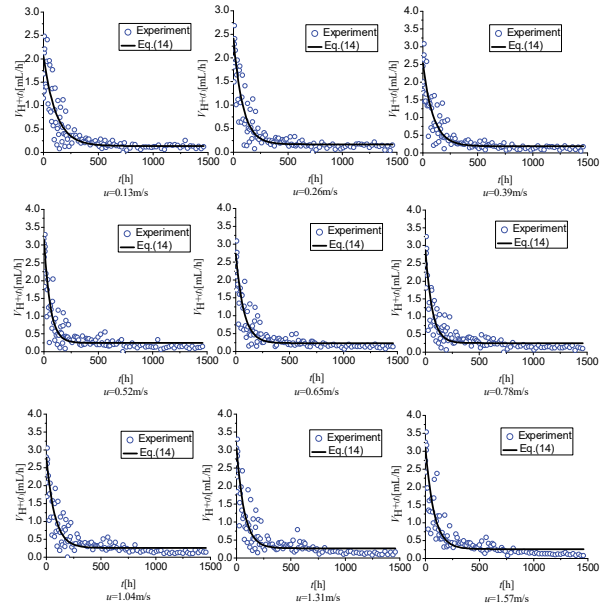


Figure 6 Acid consumption rate and fitting curves of different groups

The corrosion rates of groups are shown in Tab. 5 for 600 hours, 900 hours, 1200 hours and 1440 hours. The ratio  $R(t)$  is calculated according to Eq. (17), and the results are shown in Tab. 6.

Table 5 Acid consumption rate of the specimen at different times

Group	$u$ / m/s	$V_{H^+}(t)$ / mmol/h			
		600 h	900 h	1200 h	1440 h
1	0.13	0.0117	0.0089	0.0074	0.0068
2	0.26	0.0120	0.0092	0.0076	0.0069
3	0.39	0.0133	0.0103	0.0086	0.0077
4	0.52	0.0133	0.0106	0.0088	0.0079
5	0.65	0.0136	0.0107	0.0089	0.0080
6	0.78	0.0138	0.0110	0.0091	0.0082
7	1.04	0.0148	0.0118	0.0097	0.0087
8	1.31	0.0155	0.0118	0.0101	0.0090
9	1.57	0.0159	0.0119	0.0104	0.0092

As Tab. 6 shows, the ratio is larger than 1 when  $u_a > u_b$ , which is consistent with the result calculated by Eq. (18).

Table 6 Acid consumption rate ratio of the specimen

$R(t)$	600 h	900 h	1200 h	1440 h
$u_3/u_2$	1.023	1.030	1.027	1.024
$u_4/u_3$	1.109	1.122	1.122	1.118
$u_5/u_4$	1.004	1.026	1.022	1.022
$u_6/u_5$	1.019	1.017	1.016	1.017
$u_7/u_6$	1.014	1.025	1.019	1.017
$u_8/u_7$	1.073	1.071	1.066	1.064
$u_9/u_8$	1.047	1.004	1.042	1.030
$u_{10}/u_9$	1.036	1.066	1.021	1.014

## 4 CONCLUSIONS

A theoretical model for mortar corrosion by sulfuric acid in laminar flow is proposed and is verified by corresponding experimental study in this paper. The conclusions may be drawn as below.

(1) The corrosion rate would increase with flow velocity, but the increment effect would decrease with flow velocity in an exponential relationship, i.e. there exists an upper limit value for corrosion rate when flow velocity increases. This upper limit value is determined by concentration of sulfuric acid, diffusion coefficient of  $\text{OH}^-$ , and corrosion area of mortar when reaction is stable.

(2) Both the theoretic and experimental results indicate that the corrosion rate will quickly drop as the immersion time is going on and at last it will tend to a positive constant. The experimental relationship between corrosion and flow velocity is perfectly identical to the analytical model of corrosion rate and corrosion amount.

## Acknowledgments

This work was supported by the Natural Science Foundation of China and Yunnan Province (Grant No. 51078175).

## 5 REFERENCES

- [1] Allman, D. E. & Asisi, C. C. (1977). Asymmetric Fingerprinting based on 1-out-of-n Oblivious Transfer. *IEEE Communications Letters*, 72(11), 46-53.
- [2] Du, Y. J., Wei, M. L., Reddy, K. R. et al. (2014). Effect of acid rain pH on leaching behavior of cement stabilized lead-contaminated soil. *Journal of hazardous materials*, 14(271), 131-140. <https://doi.org/10.1016/j.jhazmat.2014.02.002>
- [3] Livingston, R. A. (2016). Acid rain attack on outdoor sculpture in perspective. *Atmospheric Environment*, 146, 332-345. <https://doi.org/10.1016/j.atmosenv.2016.08.029>
- [4] Rosso, F., Jin, W., Pisello, A. L. et al. (2016). Translucent marbles for building envelope applications: Weathering effects on surface lightness and finishing when exposed to simulated acid rain. *Construction and Building Materials*, 108, 146-153. <https://doi.org/10.1016/j.conbuildmat.2016.01.041>
- [5] Fan, Y., Zhang, S., Wang, Q., & Shah Surendra, P. (2016). The effects of nano-calcined kaolinite clay on cement mortar exposed to acid deposits. *Construction and Building Materials*, 102, 486-495. <https://doi.org/10.1016/j.conbuildmat.2015.11.016>
- [6] Chidiac, S. E. & Panesar, D. K. (2008). Evolution of mechanical properties of concrete containing ground granulated blast furnace slag and effects on the scaling resistance test at 28 days. *Cement and Concrete Composites*, 30(2), 63-71. <https://doi.org/10.1016/j.cemconcomp.2007.09.003>
- [7] Lee, H., Cody, R. D., Cody, A. M. et al. (2005). The formation and role of ettringite in Iowa highway concrete deterioration. *Cement and Concrete Research*, 35(2), 332-343. <https://doi.org/10.1016/j.cemconres.2004.05.029>
- [8] Pavlík, V., Bajza, A., Rousekova, I. et al. (2007). Degradation of concrete by flue gases from coal combustion. *Cement and concrete research*, 37(7), 1085-1095. <https://doi.org/10.1016/j.cemconres.2007.04.008>
- [9] Sun, X., Jiang, G., Bond, P. L. et al. (2014). A rapid, non-destructive methodology to monitor activity of sulfide-induced corrosion of concrete based on  $\text{H}_2\text{S}$  uptake rate. *Water Research*, 14(59), 229-238. <https://doi.org/10.1016/j.watres.2014.04.016>
- [10] O'Connell, M., McNally, C., & Richardson, M. G. (2010). Biochemical attack on concrete in wastewater applications: A state of the art review. *Cement and Concrete Composites*, 32(7), 479-485. <https://doi.org/10.1016/j.cemconcomp.2010.05.001>
- [11] Yuan, H., Dangla, P., Chatellier, P. et al. (2015). Degradation modeling of concrete submitted to biogenic acid attack. *Cement and Concrete Research*, 15(70), 29-38. <https://doi.org/10.1016/j.cemconres.2015.01.002>
- [12] Jiang, G., Sun, X., Keller, J. et al. (2015). Identification of controlling factors for the initiation of corrosion of fresh concrete sewers. *Water research*, 25(80), 30-40. <https://doi.org/10.1016/j.watres.2015.04.015>
- [13] Pavlík, V. (2007). Degradation of Concrete by Flue Gases from Coal Combustion. *Cement and Concrete Research*, 37(7), 1085-1095. <https://doi.org/10.1016/j.cemconres.2007.04.008>
- [14] Lee, H. (2005). The Formation and Role of Ettringite in Iowa Highway Concrete Deterioration. *Cement and Concrete Research*, 35(1), 332-343. <https://doi.org/10.1016/j.cemconres.2004.05.029>
- [15] Song, Z. G. & Yang, S. Y. (2007). Material Degradation of RC Structures Attacked by Acid Rain - a Field Investigation in Kunming. *Concrete*, 11(7), 23-27.
- [16] Thistlethwayte, D. K. B. (1972). Control of sulphides in sewerage systems. *Butterworth*, 7(72), 43-51.
- [17] Israel, D., Macphee, D. E., & Lachowski, E. E. (1997). Acid Attack on Pore-Reduced Cements. *Journal of Materials Science*, 32(4), 109-116.
- [18] Zhou, Q. & Hill, J. (2006). The Role of pH in Thaumassite Sulfate Attack. *Cement and Concrete Research*, 36(6), 160-170. <https://doi.org/10.1016/j.cemconres.2005.01.003>
- [19] Hewayde, E., Nehdi, M., & Allouche, E. N. (2003). Experimental Investigations of the Effect of Selected Admixture on the Resistance of Concrete to Sulfuric Acid Attack. *ASCE: Pipelines*, 14(3), 504-513.
- [20] Xie, S. D. & Li, Q. (2004). Investigation of the Effects of Acid Rain on the Deterioration of Cement Concrete Using Accelerated Tests Established in Laboratory. *Atmospheric Environment*, 38(4), 457-466. <https://doi.org/10.1016/j.atmosenv.2004.05.017>
- [21] Bohm, M. & Deviny, J. S. (1998). On a Moving-Boundary System Modeling Corrosion in Sewer Pipes. *Applied Mathematics and Computation*, 92(8), 247-269. [https://doi.org/10.1016/S0096-3003\(97\)10039-X](https://doi.org/10.1016/S0096-3003(97)10039-X)
- [22] Liu, J. & Vipulanandan, C. (2002). Modeling water and sulfuric acid transport through coated cement concrete. *Journal of engineering mechanics*, 129(4), 426-437.
- [23] Song, Z. G. & Zhang, X. S. (2011). Concentration Boundary layer Model of Mortar Corrosion by Sulfuric Acid. *Journal of Wuhan University of Technology-Mater*, 26(3), 527-532.
- [24] Schlichting, H. & Gersten, K. (2016). Extensions to the Prandtl Boundary-Layer Theory//Boundary-Layer Theory. *Springer Berlin Heidelberg*, 17(20), 377-411.
- [25] Schlichting, H. & Gersten, K. (2016). Boundary-layer theory. *Springer*, 29(32), 527-532.

### Contact information:

**Weihang ZHANG**  
Faculty of Civil Engineering,  
Kunming University of Science and Technology,  
Kunming, China

**Zhigang SONG**  
(Corresponding author)  
Faculty of Civil Engineering,  
Kunming University of Science and Technology,  
Kunming, China  
Email: songzhigang\_kust@163.com